Monitoring changes in forestry and seasonal snow using surface albedo during 1982–2016 as an indicator

Terhikki Manninen[1], Tuula Aalto[1], Tiina Markkanen[1], Mikko Peltoniemi[2], Kristin Böttcher[3], Sari Metsämäki[3], Kati Anttila[1], Pentti Pirinen[1], Ali Nadir Arslan[1]

[1]Finnish Meteorological Institute, P.O. Box 503, FI-00101, Helsinki, Finland
[2] Natural Resources Institute Finland (LUKE) P.O. Box 2, FI-00791 Helsinki,Finland
3Finnish Environment Institute (SYKE), P.O. Box 140, FI-00251, Helsinki, Finland

Correspondence to: Terhikki Manninen (terhikki.manninen@fmi.fi)

Abstract. The surface albedo time series CLARA-A2 SAL was used to study trends in the snow melt start and end dates, the melting season length and the albedo value preceding the melt onset in Finland during 1982-2016. The results were compared with corresponding snow melt timing calculated using the land ecosystem model JSBACH. In addition, the melt onset was compared with the greening-up timing based on MODIS data. Likewise the end of snow melt was compared with the melt-off day product based on Fractional Snow Cover time-series provided by Copernicus CryoLand service and the Finnish Meteorological Institute (FMI) operational end of snow melt dates based on *in situ* measurements. It was found that the albedo threshold 20 % of the melting season dynamic variation corresponded well to the melt estimate of the permanent snow layer. The greening-up followed the albedo threshold 1% within 5 – 13 days, more rapidly in mountainous areas and more slowly on coastal areas. In two northern vegetation map areas a clear trend to earlier snow melt onset (5 – 6 days per decade) and increasing melting season length (6 – 7 days per decade) was observed. In the forested part of northern Finland a clear decreasing trend in albedo (2% - 3% per decade in absolute albedo percentage) before the start of the melt onset was observed. The increased stem volume explained the trend.

1. Introduction

Surface albedo is the fraction of incoming solar radiation reflected hemispherically by the surface. It is one of the essential climate variables (ECV). It serves as an indicator of climate change and changes in the albedo also affect the climate (GCOS, 2016). Regarding the net climate effect, both land carbon budget and properties of the land surface (e.g. albedo, surface roughness) are globally significant (Davin 2010). The boreal forest zone is sensitive to changes in local and global climate and is an important component of the northern hemisphere carbon budget (Parry et al., 2007). The forest cover has a very significant influence on the northern hemisphere albedo (Bonan et al, 1992; Randerson et al., 2006). Albedo change is an important mechanism by which forests modify climate in boreal regions, but the net effect due to simultaneous change in carbon sequestration is uncertain (Betts, 2000). If the length of the snow covered season decreases and snow melts earlier in spring due to climate change, the albedo of the forest areas decreases earlier in spring, which enhances climate change. On

the other hand, if the northern forest edge moves further north due to climate change, the winter and spring time albedo will show a notable decrease, which will enhance climate change. In addition, changes in species, e.g. from deciduous (such as mountain forests typical for Arctic and Subarctic areas) to coniferous, would decrease the albedo of the snow covered season markedly. Previously it has been shown that the climatic and vegetational zones are equivalent in the boreal forests (Solantie, 2005). Hence, a marked change in climate would result in change of climatic and vegetational zones.

Already changes in land management can have a significant effect on surface temperature, equal to that of land cover change (Luyssaert et al., 2014). Changes in forest management practices can markedly affect the boreal forest albedo through changes in leaf area index, biomass or canopy density, especially in winter/spring when the forest floor is covered by snow. In Finland the forests are often managed, and the annual changes in forest biomass are monitored by the National Inventories (Tomppo et al., 2011).

In the future, the average temperature in Finland will rise more (Ruosteenoja et al., 2016a) and faster than the global average (Ruosteenoja et al., 2016b; Parry et al., 2007). Also the precipitation is estimated to increase, but more of it will be rain than snow in winter (Jylhä et al., 2012). On average the changes will be larger in winter than in summer (Ruosteenoja, 2013; Ruosteenoja et al., 2016b). Warming will be fastest in northern Finland (Ruosteenoja, 2013) and very low temperatures seem to appear rarer. However, below freezing temperatures will persist in the northern parts of the country. It is anticipated that the snow covered period will become shorter especially in southern Finland, while in northern Finland the snow cover depth may actually increase due to increased snowfall. Generally, during spring the observations indicate a larger decreasing trend in snow cover extent than the global climate models (Derksen and Brown, 2012, Thackeray et al., 2016). The variation between model results is large, and can be partly addressed to missing or over-simplified process descriptions.

Arctic warming has caused Arctic sea ice cover to decline rapidly. (Vihma, 2014). There is evidence that such a decline, together with changed heat and moisture budgets and increased snow cover in Eurasia, is connected to change towards atmospheric circulation patterns resembling the negative phase of the North Atlantic Oscillation and Arctic Oscillation, favouring cold winters in Europe and north-eastern Eurasia. According to observations, cold, snow-rich winters have become more common again in large parts of Europe since 2005 (e.g. Cohen et al. 2010, 2012, Petoukhov and Semenov 2010, Osborn 2011). Global climate models have challenges in representing the recent changes in the Arctic. The models may underestimate the observed negative Arctic Oscillation due to sea ice and snow cover changes (Handorf, 2015). The strengthening and westward shift of the Siberian high-pressure system is too weak in the models as compared to reanalysis data (Dee et al., 2011). The models have problems in the gravity wave response and upward vertical propagation (Vihma, 2014). They have not reproduced the observed winter cooling over large parts of Eurasia, and the sea ice and land surface components (or ecosystem models) of the climate models have difficulties in correct representation of the inter-annual variability of Arctic sea ice cover and terrestrial snow cover. Therefore, observations of snow and its annual cycle are needed

to discover the recent trends. Furthermore, when climate model output is used to drive a land ecosystem model to predict the evolution of snow cover, it is necessary to adjust climatic variables with observational data e.g. by means of bias correction methodologies.

5   EU Life+ MONIMET (http://www.monimet.fmi.fi) was an ambitious project spearheaded by scientists in Finland to increase turnover of climate data and to better understand climate change by mapping indicators of regional fluctuations that have an influence on the mitigation potential and vulnerability estimates of boreal forests and peatlands. The approach was based on a combination of different information sources describing phenology, CO_2 and CH_4 exchange, land cover, snow evolution and albedo (Böttcher et al., 2014; Böttcher et al., 2016). Satellite data sets provided by the MONIMET project are 10 specifically used to derive indicators for the growing season and the snow melt onset and melt-off day. MONIMET camera network was established to provide time series of vegetation (Linkosalmi et al., 2016) and snow observation (Arslan et al., 2017) and consists of about 30 cameras over Finland (Peltoniemi et al., 2018; Tanis et al., 2018).

In this work we study whether there were changes of significant scale in snow melt period and winter albedo during recent 15 decades, 1982-2016, and compare the trends to changes in forest biomass. The surface albedo data record CLARA-A2 SAL (Anttila et al., 2016a, 2016b; Karlsson et al., 2017) was used to study trends in the snow melt start and end dates, the melting season length and the albedo value preceding the melt onset. We also use snow melt-off day derived from the Copernicus CryoLand Pan-European Fractional Snow Cover time series available for years 2001 – 2016 (Metsämäki et al., 2018). The snow melt end dates operationally produced at FMI from weather station observations are used as reference data. In addition, 20 we use the land ecosystem model JSBACH (Raddatz et al., 2007; Reick et al., 2013) to derive snow melt onset and end days for the time range 1981 – 2011. The hourly climatic forcing for the land ecosystem model was produced with a regional climate model REMO (Jacob and Podzun, 1997; Jacob et al., 2001) that was constrained with ERA-interim weather (Dee et al., 2011) and further bias-corrected (Räisänen and Räty, 2013; Räty et al., 2014) with FMI gridded temperature and precipitation data (Aalto et al., 2013) to minimize the climate model inherent biases (Böttcher et al., 2016). The changes in 25 the albedo values preceding the melting season are compared with trends in the stem volume in order to evaluate, whether the changes in the forest explain the changes in albedo. The stem volume values per forest centre area obtained from the national forest inventory data sets. An albedo model (Manninen and Stenberg, 2009) is used to link stem volumes / leaf area index and albedo.

2. Materials and methods

2.1. Data sets

2.1.1. Vegetation zones

The digital vegetation zone map of Finland was provided by SYKE. The area was reduced to 13 main regions (Figure 1,

5   Table 1) by removing small islands from the map. Since the surface albedo product used in this study has a spatial resolution of only 0.25°, the removed smaller islands would cause mixed pixel problems. Even now the narrow coastal areas (Åland, Ostrobothnian coast) are prone to extra scatter due to mixed pixels. Hence, they were removed from the final analysis. The vegetation zones stretch from hemi-boreal to northern boreal.

2.1.2. Forest data

10   The forest inventory of Finland surveys forests based on a uniform and dense sampling grid, and provides unbiased estimates of forest volume, and other forest variables. The results of the inventories have been estimated for 15 forest centres (Figure 1.) in inventory reports (Korhonen et al., 2000, 2000, 2001, 2013, 2017; Salminen 1993; Salminen and Salminen 1998; Tomppo et al., 1998, 2000, 2001, 2001, 2003, 2004). In this study we compiled time series of forest volume and area estimates of forests based on published inventory reports.

The sampling system of the national forest inventory has changed from regional to continuous sampling in the past decades. In the regional sampling, the country was divided up to 15 forest centres. One or more regions (forest centres) were inventoried each year, while all regions were inventoried during the full inventory period (5-7 years). After finishing one inventory period, a new inventory period started and regions were inventoried again. More recently, in and since inventory

20   no. 10, the whole area of Finland has been inventoried within one year, but with lesser density. The full sampling density was reached within the inventory period, and forest resource estimates were again published. We assigned the forest volume estimates of newer inventories (10 and 11) to the mean years of the inventory periods. The northernmost forest centre, Lapland, further provides the estimates separately for the northern and southern parts in the most recent forest inventory.

25   The types and fraction of the forest area in each forest centre are shown in Table 2, as well as the average solar zenith angle value at melt onset time. The narrow coastal areas of Åland and Southern and Ostrobothnian coasts were removed from the analysis due to mixed pixel problems of the satellite based albedo product.

2.1.3. Snow cover melt-off data

The snow cover melt-off day used operationally at Finnish Meteorological Institute is defined to be the first day after the

30   longest period of complete snow cover in a winter, when open areas have been continuously at least half covered by snow from the day of the beginning of permanent snow cover (Solantie et al. 1996; Kersalo and Pirinen, 2009). Complete

disappearance of snow cover in open areas is reached typically 10 days later (Solantie et al., 1996). The snow melt-off days were calculated using the *in situ* snow depth measurements and the results were interpolated in a 10 km x 10 km grid.

2.1.4. Surface albedo data

The data record used in this study (CLARA-A2 SAL) covers the years 1982-2015 and is based on homogenized AVHRR data. It has been developed in the Satellite Application Facility project on Climate Monitoring, CM SAF, which is financially supported by European Organization for the Exploitation of Meteorological Satellites (EUMETSAT). The data record is described in more detail in Anttila et al. (2016a, 2016b, 2018) and Karlsson et al (2016 and 2017). The retrieved albedo is defined to wavelength range 0.25 -2.5 µm and the observations are averaged to 0.25° grid, which is also the resolution of the final product. The albedo values are given in the range 0 … 100 %. The annual mean surface albedo values preceding the onset of snowmelt were determined for the 13 regions matching the vegetation zones of Finland and for the 16 forest centre areas of Finland. Also the mean starting and end dates of the snow melt and the length of the melting season were calculated for those regions (Section 2.2.1).

2.1.5. Fractional snow cover data

At-pixel Fractional Snow Cover (FSC, % of ground area covered by snow) is extracted from pre-Copernicus Cryoland snow mapping service (Nagler et al., 2015), which provides Pan-European FSC-maps starting from 2001 at 500m (0.05°) spatial resolution. The method applied in FSC retrieval is SCAmod (Metsämäki et al., 2005; 2012), complemented by some additional NDSI (Normalized difference Snow Index) rules for detecting the snow-free areas (Metsämäki et al. 2018). SCAmod detects FSC not only for non-forested areas but is also able to capture the under-canopy snow. This type of snow product featuring 'snow on ground', not just 'viewable snow' shows high FSC if the forest floor (and under sub-canopy low vegetation) is snow-covered even though from the satellite sensor's point-of-view the forest looks darker in terms of albedo. The gained accuracy (using in-situ FSC observations at Finnish snow transects as reference) is 15-20 %-.

2.1.6. MODIS data

Daily composites of Moderate Resolution Imaging Spectroradiometer (MODIS) data for the period 2001-2016 were used for the determination of the start of growth of deciduous canopy (section 2.2.4). The Terra MODIS level-1B data were retrieved from the National Aeronautics and Space Administration (NASA)'s Level 1 and Atmosphere Archive and Distribution System (LAADS) and, from 2010 onwards, from the receiving station of the Finnish Meteorological Institute at Sodankylä. The data were processed to top-of-atmosphere (TOA) reflectances and projected into a geographic latitude/ longitude grid. The Normalized Difference Water Index (NDWI) was calculated from near-infrared (841–876 nm) and mid-infrared (1628–1652 nm) TOA-reflectances. Further details of the pre-processing are given in Böttcher et al. (2016).

2.2. Melting season start and end determination

2.2.1. Start and end day of snow melt season from surface albedo data

Previously the end of the melting season of seasonal snow has been successfully estimated using standard deviation of weekly means of albedo data (Rinne et al., 2009). Now, the CLARA-A2 SAL pentad mean albedo values were studied by fitting sigmoids matching the melting season using nonlinear regression similar to the method by Böttcher et al. 2014. For each pixel and year the pentads from end of January until end of August were used. The date of snow melt onset was taken to be the date at which the sigmoid reached 99 % of its variation range. Likewise the end of the snow melt season was defined to be the day at which the sigmoid reached 1 % of its variation range. The length of the melting season was then the difference between these two. The albedo value corresponding to the onset of melting was used as the representative albedo value preceding the melting season (Anttila et al., 2018).

At first a rough sigmoid was carried out iteratively, the maximum number of iterations being five. The reason for iteration is that the nonlinear fit outcome depends on the choice of initial parameter values of the nonlinear function to be fitted. After that, the albedo values lower than mid-sigmoid values were removed from the period preceding the melt season as temporary melt events. Likewise, possible albedo values higher than mid-sigmoid values were removed from the period succeeding the melt season as temporary snowfalls or cloud masking errors of the albedo product. Then the sigmoid was fitted anew using again a maximum of five iterations. In some areas right after the end of the snow melt new growth of vegetation started to increase the albedo level so soon that it affected the sigmoid fitting. Therefore the minimum albedo value starting from the mid-sigmoid was sought. A second order polynomial was fitted to the part of the albedo curve starting from that point. This regression polynomial was used to remove the growth season increase of the albedo but leave the pointwise variation of that part of the original curve (i.e. in Figure 2 the blue curve of original data is replaced with the black curve in further nonlinear fitting). The updated albedo curve was then used as the basis of a new sigmoid fit with maximum number of iterations being five. If the value of the coefficient of determination R^2 was smaller for the second sigmoid fit than for the first fit and R^2 was smaller than 0.99 for the first fit, the latter sigmoid fit was carried out anew with the maximum number of iterations being now increased to 15. Finally the sigmoid of the two rounds that had on the average smallest fit residuals was chosen.

In some cases the snow melt onset could not be determined, because it had started already before the first cloud free albedo pentad was available for the pixel and year in question. For the regional mean values of the melt onset and end dates and albedo at the melt onset day, only the pixels for which the melt onset day was available were included in the analysis.

2.2.2. Start and end day of snow melt season from Ecosystem model

JSBACH land surface model (Raddatz et al., 2007; Reick et al., 2013) resolves land surface physical and biogeochemical processes involved in surface energy balance as well as water and carbon balances within soil and vegetation. In addition to

its principal use to serve as a land surface boundary for the Max Planck Institute for Meteorology Earth System Model (MPI–ESM) (Stevens et al., 2013), JSBACH can be driven with prescribed weather data. In this work JSBACH was driven using the bias corrected hourly REMO data for the years 1980–2011 with a spin-up period of 30 years before the forward run to equilibrate soil water and soil temperature. The spatial domain of JSBACH is also Fennoscandia in a resolution of 0.167°, but in the present study only Finnish territory is investigated.

The JSBACH set-up used requires seven mutually consistent meteorological drivers: 2-m air temperature (Tair) and specific humidity, 10-m wind velocity, short-wave and long-wave radiation, potential short-wave radiation and precipitation (Pr) prescribed in hourly time resolution. For providing these drivers we used the regional climate model REMO (Jacob and Podzun, 2007; Jacob et al., 2011) with an implementation of surface properties by Gao et al. (2015). The modelling domain for REMO was Fennoscandia, with a grid resolution of 0.167°, corresponding approximately to 18 km. Lateral boundary data was taken from ERA-Interim, a global atmospheric re-analysis produced by the European Centre for Medium- Range Weather Forecasts (ECMWF) (Dee et al., 2011). The forward run covered the period from 1979 to 2011 and it was preceded by a 10-yearspin-up to equilibrate soil moisture and temperature.

Model-specific biases are inherent for regional climate models (Christensen et al., 2008; Teutschbein & Siebert, 2012) and it is known that REMO exhibits too cold winter temperatures in an Eastern European area that covers most of Finland (Pietikäinen et al., 2012; Gao et al., 2015). The modelled summer and autumn temperatures tend to exceed observations. Moreover, REMO overestimates precipitation in northern Europe throughout the year. To account for the biases, we adjusted air temperature and precipitation against gridded homogenized weather data for 1980–2011 provided by the Finnish Meteorological Institute (FMI) (Aalto et al., 2013) using a quantile–quantile type bias correction algorithm for daily mean temperature (Räisänen and Räty, 2013), while daily cumulative precipitation was adjusted using parametric quantile mapping (Räty et al., 2014). Finally, the daily corrections were applied to the hourly modelled air temperature and precipitation values.

In JSBACH surface grid cells are divided into fractions of four most prevalent plant functional types (PFT) that are characterised with properties such as maximum leaf area, phenology type, growth rate, shedding rate and photosynthesis parameters. In addition to PFT fractions, each grid cell is characterised with a maximum fraction of the land area that is hospitable to plants.

Snowfall fraction of the total precipitation is given as follows:

$$Pr\_sn = \begin{cases} 0, & Tair > 3.3°C \\ Pr * (3.3° - Tair)/4.4°, & -1.1°C < Tair < 3.3°C \\ Pr, & Tair < -1.1°C \end{cases} \tag{1}$$

Pr_sn is further distributed to surface and canopy reservoirs with the constant fraction of 0.25 to be intercepted by the canopy. In addition to the snowfall fraction the fate of the canopy reservoir is constrained by sublimation and unloadings due to melting that is temperature regulated and due the wind-blow (Roesch et al., 2001). Furthermore the accumulation of snow is limited by leaf area index. At the ground the snow budget composed of the excess snowfall fraction after canopy interception, sublimation and melting.

The snow depth was used as an indicator of the melting season start and end. During early spring the changes in model albedo are very strongly dominated by changes in snow cover, since the changes in the leaf area of the coniferous forest are minor and the bud burst of broadleaved forest occurs later in spring. The modelled melting season timing and duration were studied by fitting a sigmoid to each grid cell of the yearly spring time snow depth data. The fit was done in two phases: first sigmoid was fitted between days of year 30 and 200 to include days of yearly maximum and minimum snow cover. As modelled snow cover did not typically show a plateau before the start of the melt period, but tended to increase monotonously until the start of the melting, values lower than the first fit were rejected from the part of the time-series prior to the point where sigmoid reaches its half of the range value. If fewer than 15 data points were left after the rejection, the grid cell in that year was rejected. Otherwise sigmoid was fitted to the remaining data series. After the second fit a sanity check was made to reject the fittings implying either too small or too large difference between the sigmoid parameter values representing the snow cover levels before and after the melting. Because the snow melt starts rather gradually and ends abruptly in the modelled snow depth data, asymmetric criteria of 98% and 8% of the sigmoid variation range was used for the start and end dates of the melting period, respectively. Finally, for each vegetation zone yearly regional means of start and end days were calculated.

2.2.3. Snow melt-off day from Fractional snow cover data

The detection of snow melt-off day from the FSC map time series provides for each pixel the first day with snow-free terrain, but ignores short (a few days) intervening snow-free periods within a long snow season (Metsämäki et al. 2018). The melt-off day from the FSC time series is identified as a beginning of a snow-free period (FSC = 0%) after a period of snow observations (FSC > 0%). A pixel is assigned the status "melted" after a period of at least six subsequent snow-free days is found (however with possible intervening cloudy observations), if the number of the snow-free days represents 80% of all cloud-free observations after the first day of the snow-free period in concern. The first day of this period is accepted as a candidate for the melt-off day. After the candidate day, a "new snow period" is allowed, if at least three subsequent snow days are observed. Then a new search for melt-off day is launched the same way as before.

2.2.4. Starting of growth season of deciduous canopy from MODIS data

The start of the growing season of deciduous vegetation in Finland, usually referred to as greening-up, was determined from NDWI using the method described in Böttcher et al. (2016). The NDWI was utilized because the detection of the greening-up in boreal areas from the Normalized Difference Vegetation Index (NDVI) can be affected by melting of snow, whereas the NDWI allows a differentiation between snow melt and greening-up (Delbart et al., 2006). The start of the growing season showed good correspondence with the date of birch bud break (RMSE of one week) at Finnish phenological sites when the corresponding MODIS pixels are dominated by deciduous forest. The data set for the period 2001−2016 has a spatial resolution of 0.5×0.5 degrees.

2.2.5. Albedo model calculations

The effect of snow cover on surface albedo of coniferous forests can be estimated using an albedo model based on photon recollision probability (Manninen and Stenberg, 2009). The forest parameters required are the leaf area index (LAI), the clumping factor and the single scattering albedo of needles. In addition, the sun zenith angle value is needed. The average value of the sun zenith angle of the forest centres at the start day of snow melt was used in the calculations (Table 2). The snow cover of the forest floor is described using its albedo. The forest inventory does not contain LAI information and a strong relationship between the stem volume and LAI can't be expected at high spatial resolution. Yet, in larger areas one could assume that LAI of a forest is statistically related to the stem volume per area V according to LAI $= k \, V^{2/3}$. When comparing the albedo simulations to the satellite measurements in a larger area, one has to take into account also the fraction of forested area. The albedo was simulated in the forest centre areas for the years matching the national forest inventory during 1963 − 2011 varying the coefficient k in the range 0.1…1.5. The optimal value of k was defined to be the value corresponding to smallest difference between the simulated and satellite based albedo values. It turned out that there was a relatively strong relationship between the optimal value of k and the fraction of the forest area in the boreal forest zone (Figure 3). The area left outside the regression (Northern Lapland) is dominated by deciduous species (mountain birch), hence its LAI value in winter is not related to the stem volume similarly as for the coniferous species.

3. Results

3.1. Seasonal snowmelt timing

3.1.1. Snow melt onset

The onset of melting was determined using the sigmoids determined both from the satellite based albedo data CLARA-A2 SAL pentads and the daily JSBACH model calculations of the snow depth. The comparison of these melting season start dates is shown in Figure 4. The overall agreement is good, and some of the scatter can be attributed to using a different variable for the data (albedo) and the model (snow depth). For the model calculations the snow depth was used as the

indicator of the snow melt onset rather than the albedo, because the snow depth is more related to the snow accumulation throughout the seasonal cold period, whereas albedo is sensitive to the prevailing weather conditions before the melt onset. Snow depth describes the whole snowpack, whereas the albedo describes only the topmost layer of it. The surface albedo product showed a negative trend (about half a day per year) in two areas: Northern Karelia – Kainuu and Southwestern Lapland (Table 3, Figure 5). For the other areas the coefficient of determination for a linear trend of five year average values was smaller than 0.5. The annual variation of the melt onset day is so large (standard deviation being on the average 12 days for the time range 1982-2015) that it easily masks a long term trend. This was even more evident in the land ecosystem model calculation results, where a low frequency variation dominated the time window so that no area showed a marked trend even in the five year moving average curve. Especially variable melt onset timing is in the coastal regions (Southwestern Finland and Southern Ostrobothnia) and in the Lake district. For those regions the standard deviation values of the melt onset day are 14.3, 14.7 and 14.6, respectively. For the Northern Fjeld Lapland the vicinity of the Barents Sea obviously causes also higher a standard deviation (13.4) of the melt onset day. So large part of Finland is coastal that changes in air temperature or precipitation preceding melt onset are not that directly dominating as in some regions of the northern hemisphere (Anttila et al., 2018), but the sea ice extent of the Baltic Sea has a large effect as well. When using 10 year moving averages for the trend analysis based on albedo data, a negative trend ($R^2 > 0.5$) of melt onset day was detected in Northern Karelia – Kainuu, Southwestern Lapland, Ostrobothnia, Kuusamo district and Lake district. Although the time series of 34 years is not really long enough for using 10 year averages, the results, however, confirm the intuitive impression that the snow melt starts earlier than it used to do in the past, as the two distinct areal trends showed.

3.1.2. End of snow melt

The end of snow melt was determined using the albedo data, the snow depth value of the land ecosystem model and the snow melt-off day derived from the satellite based fractional snow cover estimate for each area of the vegetation zone map. The results were compared with the FMI snow melt maps provided operationally by the climate service of FMI (Solantie et al., 1996; Figure 6). The overall agreement is good for the melt-off day derived from MODIS-based FSC and the FMI operational melt-off-day derived using *in situ* data taking into account that the satellite based melt-off date refers to completely snow-free case, whereas the *in situ* based melt-off date refers to the end of the permanent snow cover, when half of open areas still have snow (Figure 6). The 1 % threshold for the albedo produced a clearly later end of melt day than the *in situ* based snow melt-off day and model results. This is understandable, because the FMI operational melt-off day is not yet completely snow-free and the albedo value is very sensitive to even small amounts of snow. It turned out that the day at which the albedo based sigmoid reached 20% of its variation range matched well the official end date of snow melt and the value 15% matched well the FSC based melt-off day. The difference between dates corresponding to the 20% and 1% threshold values of the albedo based sigmoids is of the order of 13 days, which is in line with the 10 days difference during which half snow free open areas become completely snow free (Solantie et al., 1996). Results from JSBACH coincide well with the operational end of permanent snow cover. Probably the snow-off bias inherited from the climate model surface

parametrizations explain why the zero value of snow depth of JSBACH matches the time, when half of open areas are snow-free. It has been shown that e.g. in ECHAM5 the snowmelt occurs at too low temperatures (Räisänen et al., 2014). Consequently, too much of the surface net radiation is consumed in melting snow and too little in heating the air.

5   No systematic trend was observed for the end of snow melt day for albedo or land ecosystem model data. It seems that the onset of snowmelt depends more clearly on the climate and the end of snowmelt is more sensitive to the prevailing weather conditions at that time.

The aerial advance of spring is demonstrated by the FMI operational melt-off map, the surface albedo 20 % threshold map,
10   the FSC melt-off map and the greening-up map in years 2006 and 2012 (Figure 7). The general agreement is good, and the overall zones of equal timing are obvious.

3.1.3. Length of melting season of snow

The length of the melting season was determined as the difference between the dates corresponding to the end of the snow melt and the onset of the snow melt. The 99 % and 1 % threshold values were used for the albedo sigmoids. A clear trend of
15   increasing melting period length was observed in the areas, Northern Karelia – Kainuu and Southwestern Lapland, where the snow melt starts earlier than before (Table 3, Figure 8). For the length of the melting season the standard deviation during 1982-2015 was on the average, naturally, even larger than for the melt onset day the value being as high as 16 days. The largest values occurred again in Southwestern Finland (20.3), Southern Ostrobothnia (17.5), Lake district. (17.1) and Northern Fjeld Lapland (20.0). When using 10 year moving averages in the trend analysis, the result was that the melting
20   season length increased in Northern Karelia – Kainuu, Kuusamo district, Southwestern Lapland and North Ostrobothnia and decreased in Northern Fjeld Lapland.

3.2. Starting of the growing season

The start of the growing season of deciduous vegetation based on MODIS NDWI values turned out to almost coincide with timing of the 1% threshold value of the surface albedo, being only slightly later (Figure 6). This is probably due to the large
25   fraction of deciduous species being in open areas and on the forest floor, which start growing only after the soil has become completely snow free and even small amounts of remaining snow have a large effect on the albedo. The 16 year average time between the date, when the SAL value reached 1% of its dynamic range during the melting season, and the date of the greening-up varied in the vegetation zones between 5 and 13 days. The largest difference took place on the coast and the shortest in mountain areas, where greening of mountain birch can occur even before snow melt (Shutova et al., 2006). In
30   addition, trees in the northern boreal region have a lower temperature requirement for budburst than in the south and day length is already longer in the north at the time of budburst. Therefore, the intensity of response to temperature increases

from south to north and observed trend to earlier budburst was stronger in the northern boreal zone compared to the southern boreal zone for the period 1997-2006 (Pudas et al., 2008).

3.3. Albedo before onset of snow melt

The surface albedo at the melt onset shows a decreasing trend in several northern regions based on vegetation zones (Table 4, Figure 9). This can be explained by the increase in stem volume, as the albedo model results agree with the observed albedo trends of the forest centre based regions (Table 5, Figure 10). It is obvious also that meaningful trends ($R^2 > 0.5$) for five year average albedo values were obtained only when the fraction of forested area exceeded 0.7 and the stem volume was smaller than 75 m^3/ha. For those areas (Southern Lapland, Kainuu, Northern Ostrobothnia, Lapland and North Karelia) the albedo trend is negative. It is well known that the winter time albedo depends strongly on the LAI (and thus stem volume of a larger area), when the LAI is relatively small (Manninen and Stenberg, 2009). For larger LAI values the albedo more or less saturates and a further increase of LAI does not show up markedly. As expected, no clear albedo trend after the snow melt was observed. The reason is that the difference between the canopy and forest floor albedo is not significant, whereas the snow and canopy albedo values differ markedly. Hence, the accumulating stem volume in the northern part of Finland causes darkening of the winter/spring time albedo, but does not have a significant effect on the albedo value right after the snow melt.

4. Discussion

Surface albedo is determined by the quantity and type of land vegetation, the seasonal cycle of leaf development, and the existence of snow cover. The snow conditions also depend on the vegetation cover. Seasonal dynamics of snow and vegetation are driven by temperature and precipitation. The air temperatures in the Arctic and boreal regions have increased and Arctic sea ice cover has reduced, and the influences can be seen in Finnish temperature and precipitation records. The trends are not self-evident, although as a whole the arctic/boreal region is changing towards warmer climate. The large variation in the climate can be seen in both observed and modelled snow melt onset. The observed trends are clearly negative only in Northern Carelia – Kainuu and North Ostrobothnia. The year-to-year variation in the modelled onset is not as large as in the observed onsets but the multi-year variation is similar, model acting as a smoother of observations. In many cases, both positive and negative tendencies appear during the study period, most significantly in around year 2000, when the snow melt showed a transition from earlier onset to later onset in Southwestern Finland, Lake district and Ostrobothnia. Also a previous analysis using 35 years data set from passive microwave radiometer snow clearance dataset, Metsämäki et al. (2018) concluded that snow melt-off at northern latitudes in Europe has advanced 3-5 days per decade for boreal forests and tundra. The MODIS FSC-based snow melt-off maps gave a similar signal.

The trends in end of snow melt are insignificant everywhere. However, combined with negative snow melt onset trend in Northern Carelia – Kainuu and North Ostrobothnia, we obtain an increase of length of snow melt period in those regions. Generally, in northern latitudes, many studies have shown persistent negative trends in snow melt and positive trends in early spring vegetation activity (Myneni et al., 1997; Pulliainen et al., 2017). A recent study indicated increase in the length of snow melt period (Contosta, 2017), which could have both negative and positive impacts to e.g. soil water availability, nitrogen cycling and ecosystem carbon and energy balance and thus induce complex perturbation of land surface – climate feedbacks.

The forest growth in Finland can be linked in forest centre resolution to the sum of effective temperatures, the frost sum and the mean snow depth during the winter in a very robust way (Solantie 2015). The snow cover affects directly the winter greatest soil frost depth. According to Solantie (2015) most of the increase in the growth-rate in forest stands in the southern half of Finland during 1961-2010 is caused by a change in climate. The snow cover affects the roots of the trees via the soil frost. In regions of deep soil frost the roots tend to concentrate in the surface layer, otherwise deeper down. Changes in snow cover are hence expected to affect also the amount of wind throw. In warming climate the roots will concentrate deeper down and then in summer the canopy will tolerate higher wind speeds than before in otherwise similar conditions. On the contrary, late autumn, winter and early spring storms will be more dangerous for the canopy, if the soil is not frozen as it used to be in the past (Peltola et al., 1999). The traffictability of the forested terrain may reduce with earlier snow melt (Kellomäki et al., 2010).

The timber resources in Finnish forests have grown since the 1950's more than has been removed by logging (National Forest Inventory, 2013). In northern Finland the share of stout timber has traditionally been high, so that the increase comes mainly from small-diameter timber. While carbon storage in forests has increased Finland has darkened, which shows in the negative trend of albedo preceding snow melt season. The effect of canopy on snow covered terrain albedo is largest for small LAI values (Jääskeläinen and Manninen, 2018), hence it is understandable that the marked decreasing trend of albedo before snow melt season is observed in northern Finland. In southern Finland the share of stout timber has more than quadrupled since the 1950's, yet no trend in pre-melt albedo during 1982-2016 is observed there. Hence, the idea to increase carbon sinks in forests by increasing the timber resources of existing forests by causing trees to grow more densely and become stouter (Pihlainen et al., 2014; Baul et al., 2017a, 2017b; Pingoud et al., 2018) suggests a possibility to combat climate change in regions of already medium size canopy without the negative albedo feedback.

5. Conclusions

The surface albedo proved to be a suitable indicator of the melt onset and end of melting season. Overall agreement was found with corresponding dates determined using the JSBACH land ecosystem model snow depth data. The operationally

provided end of permanent snow cover date based on *in situ* data corresponded to about the day when that surface albedo value reached the lower 20% of its dynamic range during the melting season. The end of snow melt determined using satellite based fractional snow cover data and JSBACH land ecosystem model snow depth data also agreed well with the corresponding operationally produced date. The day, when the surface albedo has decreased to the lower 1 % of its dynamic

5   range is well in line with the day corresponding to completely snow free open areas. In addition, the greening-up day followed on the average 5 – 13 days later.

According to the albedo data, the melt onset day has advanced by about 17 and 21 days, i.e. 5 and 6 days per decade, respectively, in two regions in northern Finland (North Ostrobothnia and Northern Karelia - Kainuu), respectively. Likewise

10 in those areas the length of melting season has increased by 23-24 days, i.e. 7 days per decade. The albedo data also shows darkening albedo values (2% - 3% per decade in absolute albedo percentage) preceding the snow melt onset in North Ostrobothnia, Northern Karelia, Kainuu and Lapland, especially in Southern Lapland, which is coniferous species dominated. This albedo decrease could be explained by the observed increase in stem volume in those areas.

15 **Data availability**

The surface albedo data is available at the web user interface of CM SAF project: https://wui.cmsaf.eu/safira/action/viewProduktSearch;jsessionid=5137E8E5FEF904478BBC386333FD8EB0.ku_2. The data on the start of the growing season (greening-up of deciduous vegetation) for the period 2001-2016 data can be viewed online in a web map application (http://syke.maps.arcgis.com) is and are available for download at the Open data service of SYKE

20 (http://www.syke.fi/en-US/Open_information/Spatial_datasets#P). The original FSC data is available from the Cryoland portal (http://neso1.cryoland.enveo.at/cryoclient/). Forest inventory data is not publicly available, but aggregated values are (http://kartta.luke.fi/index-en.html).

Author contributions

TeM performed the albedo data analysis, comparison with other data sets and albedo modelling. TiM carried out the

25 ecosystem model calculations and analysis of those results. TA planned and led the climate related work and interpreted the simulation results. MP provided the forest inventory data, KB provided the greening-up data, SM provided the FSC-based yearly melt-off day data, KA provided the albedo data and PP provided the FMI snow melt data. AN coordinated the Monimet project and everybody participated in the scientific discussions. All authors participated in the writing of the paper.

Acknowledgements

The authors are grateful for EUMETSAT for financial support to generate the CLARA-A2 SAL time series in the CM SAF project. Life+ project Monimet (Grant agreement LIFE12 ENV/FI000409). The authors are grateful to Mr. Achim Drebs for discussions related to snow melt. The authors wish to thank also Ms. Maria Holmberg and Ms. Katri Rankinen for their co-operation at various phases of the project and for providing the vegetation zone map. We thank the Academy of Finland Center of Excellence (307331), OPTICA (295874) and CARB-ARC (285630) for support.

References

Aalto, J., Pirinen, P., Heikkinen, J. and Venäläinen, A: Spatial interpolation of monthly climate data for Finland: comparing the performance of kriging and generalized additive models, Theoretical and Applied Climatology, 112, 99-111, 2013.

Anttila, K., Jääskeläinen, E., Riihelä, A., Manninen, T., Andersson, K. and Hollman, R.: Algorithm Theoretical Basis Document: CM SAF Cloud, Albedo, Radiation data record ed. 2 – Surface Albedo, 85 pp, Doi:10.5676/EUM_SAF_CM/CLARA_AVHRR/V002, 2016a.

Anttila, K., Jääskeläinen, E. , Riihelä, A., Manninen, T., Andersson, K. and Hollman, R.: Validation Report: CM SAF Cloud, Albedo, Radiation data record ed. 2 – Surface Albedo, 54 pp, DOI: 10.5676/EUM_SAF_CM/CLARA_AVHRR/V002, 2016b.

Anttila, K., Manninen, T., Jääskeläinen, E., Riihelä, A., and Lahtinen, P.: The Role of Climate and Land Use in the Changes in Surface Albedo Prior to Snow Melt and the Timing of Melt Season of Seasonal Snow in Northern Land Areas of 40 N–80 N during 1982–2015, Remote Sensing, 10, 1619; 2018. Arslan, A., Tanis, C., Metsämäki, S., Aurela, M., Böttcher, K., Linkosalmi, M. and Peltoniemi, M.: Automated Webcam Monitoring of Fractional Snow Cover in Northern Boreal Conditions, Geosciences, 7, 55, doi:10.3390/geosciences7030055, 2017.

Baul, T.K., Alam, A., Ikonen, A., Strandman, H., Asikainen, A., Peltola, H. and Kilpeläinen, A.: Climate Change Mitigation Potential in Boreal Forests: Impacts of Management, Harvest Intensity and Use of Forest Biomass to Substitute Fossil Resources. Forests, 8, 455; doi:10.3390/f8110455, 2017a.

Baul, T.K. Alam, A., Strandman, H. and Kilpeläinen, A.: Net climate impacts and economic profitability of forest biomass production and utilization in fossil fuel and fossil-based material substitution under alternative forest management. Biomass and Bioenergy 98, 291-305, 2017b.

Betts R.A.: Offset of the potential carbon sink from boreal forestation by decreases in surface albedo, Nature, 408, 187–190, 2000.

Bonan, G.B.; Pollard, D.; Thompson, S.L.: Effects of boreal forest vegetation on global climate, Nature, 359, 716-718, 1992.

Böttcher, K., Aurela, M., Kervinen, M., Markkanen, T., Mattila, O.-P., Kolari, P., Metsämäki, S., Aalto, T., Arslan, A.N. and Pulliainen, J.: MODIS time-series-derived indicators for the beginning of the growing season in boreal coniferous forest —

A comparison with CO2 flux measurements and phenological observations in Finland, Remote Sensing of Environment, 140, 625-638, 2014.

Böttcher, K., Markkanen, T., Thum, T., Aalto, T., Aurela, M., Reick, C., Kolari, P., Arslan, A., & Pulliainen, J.: Evaluating biosphere model estimates of the start of the vegetation active season in boreal forests by satellite observations. Remote Sensing, 8, 580, 2016.

Contosta, A.R., Adolph, A., Burchsted, D., Burakowski, E., Green, M., Guerra, D., Albert, M., Dibb, J., Martin, M., McDowell, W.H., Routhier, M., Wake, C., Whitaker, R. and Wollheim, W.: A longer vernal window: the role of winter coldness and snowpack in driving spring transitions and lags, Glob Chang Biol., 23(4), 1610-1625. doi: 10.1111/gcb.13517, 2017.

Christensen, J.H.; Boberg, F.; Christensen, O.B.; Lucas-Picher, P.: On the need for bias correction of regional climate change projections of temperature and precipitation. Geophysical Research Letters, 35, L20709, 2008.

Cohen J., Foster J., Barlow M., Saito K., Jones J.: Winter 2009–2010: a case study of an extreme Arctic Oscillation event, Geophys. Res. Lett. 37:GL044256, 2010.

Cohen, J.L., Furtado, J.C., Barlow, M.A., Alexeev, V.A., Cherry, J.E.: Arctic warming, increasing snow cover and widespread boreal winter cooling, Environ Res Lett 7:014007. doi:10.1088/1748-9326/7/1/014007, 2012.

Davin, E. L. and de Noblet-Ducoudré, N.: Climatic impact of global-scale deforestation: Radiative versus nonradiative processes, J. Climate, 23, 97–112, 2010.

Dee, D.P., Uppala, S.M., Simmons, A.J., Berrisford, P., Poli, P., Kobayashi, S., Andrae, U., Balmaseda, M.A., Balsamo, G., Bauer, P., et al.: The ERA-Interim reanalysis: configuration and performance of the data assimilation system, Quarterly Journal of the Royal Meteorological Society, 137, 553-597, 2011.

Delbart, N., Le Toan, T., Kergoat, L., and Fedotova, V.: Remote sensing of spring phenology in boreal regions: A free of snow-effect method using NOAA-AVHRR and SPOT-VGT data (1982-2004), Remote Sensing of Environment, 101, 52-62, 2006.

Derksen, C. and Brown, R.: Spring snow cover extent reductions in the 2008 – 2012 period exceeding climate model projections, Geophys. Res. Letters, 39, L19504, 6p., 2012.

Gao, B.-C.: NDWI-A normalized difference water index for remote sensing of vegetation liquid water from space. Remote Sensing of Environment, 58, 257-266, 1996.

Gao, Y., Weiher, S., Markkanen, T., Pietikäinen, J.-P., Gregow, H., Henttonen, H.M., Jacob, D. and Laaksonen, A.: Implementation of the CORINE land use classification in the regional climate model REMO, Boreal Environmental Research, 20, 261-282, 2015.

Handorf, D., R. Jaiser, K. Dethloff, A. Rinke, and J. Cohen: Impacts of Arctic sea ice and continental snow cover changes on atmospheric winter teleconnections, Geophys. Res. Lett., 42, 2367–2377, doi:10.1002/ 2015GL063203, 2015.

Jacob, D. and Podzun, R.: Sensitivity studies with the regional climate model REMO, Meteorology and Atmospheric Physics, 63(1), 119-129, 1997.

Jacob, D., Van den Hurk, B.J.J.M, Andrae, U., Elgered, G., Fortelius, C., Graham, L.P., Jackson, S.D., Karstens, U., KoÈpken, Chr., Lindau, R., Podzun, R., Rockel, B., Rubel, F., Sass, B.H., Smith, R.N.B., and Yang, X.: A comprehensive model inter-comparison study investigating the water budget during the BALTEX-PIDCAP period, Meteorology and Atmospheric Physics, 77(1-4), 19-43, 2001.

5 Jylhä, K., Ruosteenoja, K., Räisänen, J. and Fronzek, S.: Ilmasto. In: Ruuhela, R. (Ed.), Miten väistämättömään ilmastonmuutokseen voidaan varautua? - yhteenveto suomalaisesta sopeutumistutkimuksesta eri toimialoilla, (In Finnish), Maa- ja metsätalousministeriö, Helsinki. MMM:n julkaisuja 6/2011, 16–23, 2012.

Karlsson, K.-G., Anttila, K., Trentmann, J., Stengel, M., Meirink, J. F., Devasthale, A., Hanschmann, T., Kothe, S., Jääskeläinen, E., Sedlar, J., Benas, N., van Zadelhoff, G.-J., Schlundt, C., Stein, D., Finkensieper, S. and Håkansson, N.:
10 GCOS: The Global Observing System for Climate: Implementation needs, Reference Number GCOS-200, WMO, 315 pp., 2016.

Karlsson, K.-G., K. Anttila, J. Trentmann, M. Stengel, J. F. Meirink, A. Devasthale, T. Hanschmann, S. Kothe, E. Jääskeläinen, J. Sedlar, N. Benas, G.-J. van Zadelhoff, C. Schlundt, D. Stein, S. Finkensieper, N. Håkansson, and R. Hollmann: CLARA-A2: the second edition of the CM SAF cloud and radiation data record from 34 years of global AVHRR
15 data. Atmos. Chem. Phys., 17(9), 5809-5828, 2017.

Kellomäki, S., Maajärvi, M., Strandman, H., Kilpeläinen, A. and Peltola, H.: Model computations on the climate change effects on snow cover, soil moisture and soil frost in the boreal conditions over Finland. Silva Fennica, 44(2), 213–233, 2010.

Kersalo, J. and Pirinen, P., (Eds.), Suomen maakuntien ilmasto (in Finnish with English summary), Finnish Meteorological
20 Institute Reports, 2009:8, 192 p., 2009.

Korhonen, K.T., Tomppo, E., Henttonen, H., Ihalainen, A. and Tonteri, T.: Hämeen-Uudenmaan metsäkeskuksen alueen metsävarat 1965–99 (In Finnish). Metsätieteen aikakauskirja 3B/2000: 489–566, 2000.

Korhonen, K.T., Tomppo, E., Henttonen, H., Ihalainen, A., Tonteri, T. and Tuomainen, T.: Pirkanmaan metsäkeskuksen alueen metsävarat 1965–1999 (In Finnish). Metsätieteen aikakauskirja 4B/2000: 661–739, 2000.

25 Korhonen, K.T., Tomppo, E., Henttonen, H., Ihalainen, A., Tonteri, T. and Tuomainen, T.:. Pohjois-Karjalan metsäkeskuksen alueen metsävarat 1966–2000 (In Finnish). Metsätieteen aikakauskirja 3B/2001: 495–576, 2001.

Linkosalmi, M., Aurela, M., Tuovinen, J.-P., Peltoniemi, M., Tanis, C. M., Arslan, A. N., Kolari, P., Aalto, T., Rinne, J. and Laurila, T.: Digital photography for assessing vegetation phenology in two contrasting northern ecosystems, Geosci. Instrum. Meth., 1–25, doi:10.5194/gi-2015-34, 2016.

30 Luyssaert S., Jammet, M., Stoy, P.C., Estel, S., Pngratz, J., Ceschia, E., Churkina, G., Don, A., Erb, K.H., Ferlicoq, M., Gielen, B., Grünwald, T., Houghton., R.A., Klumpp, K., Knohl, A., Kolb, T., Kuemmerle, T., Laurila, T., Lohila, A., Loustau, D., McGrath, M., Meyfroidt, P., Moors, E.j., Naudts, K., Novick, K., Otto, J., Pilegaard, K., Pio, C.A., Rambal, S., Rebmann, C., Ryder, J., Suyker, A.E., Varlagin, A., Wattenbach, M. and Dolman, J.: Land management and land cover change have impacts of similar magnitude on surface temperature, Nature Clim. Change. doi:10.1038/nclimate2196, 2014.

Manninen, T. and Jääskeläinen, E.: The effect of boreal forest canopy on snow covered terrain broadband albedo, submitted for publication in Geophysica, 2018.

Manninen, T. and Stenberg, P.: Simulation of the effect of snow covered forest floor on the total forest albedo, Agricultural and Forest Meteorology, 149(2), 303-319, 2009.

5 Metsämäki, S., Anttila, S., Huttunen, M., and Vepsäläinen, J.: A feasible method for fractional snow cover mapping in boreal zone based on a reflectance model, Remote Sensing of Environment, 95, 77–95, 2005.

Metsämäki, S., Mattila, O.-P., Pulliainen, J., Niemi, K., Luojus, K., Böttcher, K.: An optical reflectance model-based method for fractional snow cover mapping applicable to continental scale, Remote Sensing of Environment, 123, 508-521, 2012.

Metsämäki, S., Böttcher, K., Pulliainen, J., Luojus, K., Cohen, J., Takala, M., Mattila, O.-P., Schwaizer, G., Derksen, C., and

10 Koponen, S.: The accuracy of snow melt-off day derived from optical and microwave radiometer data — A study for Europe. Remote Sensing of Environment, 211, 1-12, 2018.

Myneni, R. B., Keeling, C. D., Tucker, C. J., Asrar, G. and Nemani, R. R.: Increased plant growth in the northern high latitudes from 1981 to 1991, Nature, 386, 698–702, 1997.

National Forest Inventory, Finnish Forest Research Institute 2013.

15 Nagler, T. Bippus, G., Schiller, C., Metsämäki, S., Mattila, O.-P., Luojus, K., Malnes, E., Solberg, R., Diamandi, A., Larsen, H.E., Wiesmann, A., Gustafsson, D., 2015. CryoLand - Copernicus Service Snow and Land Ice: Final Report, pp. 46.available at http://cryoland.eu and http://enveo.at.

Osborn, T.J.: Winter 2009/2010 temperatures and a record-breaking North Atlantic Oscillation index, Weather 66:19–21, 2011.

20 Parry, M.L., Canziani, O.F., Palutikof, J.P., van der Linden, P.J. and Hanson, C.E.: IPCC: Climate Change 2007: Impacts, Adaptation and Vulnerability, Contribution of Working Group II to the Fourth Assessment Report of the Intergovernmental Panel on Climate Change, Cambridge University Press: Cambridge, London, UK, 976 pp., 2007.

Peltola, H., Kellomäki, S. and Väisänen, H.: Climatic Change, 41(17). https://doi.org/10.1023/A:1005399822319, 1999.

Peltoniemi, M., Aurela, M., Böttcher, K., Kolari, P., Loehr, J,; Karhu, J., Linkosalmi, M., Tanis, C. M., Tuovinen, J.-P. and

25 Arslan, A. N.: Webcam network and image database for studies of phenological changes of vegetation and snow cover in Finland, image time series from 2014 to 2016, Earth Syst. Sci. Data, 10, 173–184, doi:10.5194/essd-10-173-2018, 2018.

Petoukhov V. and Semenov, V.A.: A link between reduced Barents-Kara sea ice and cold winter extremes over northern continents, J Geophys Res 115:D21111, 2010.

Pietikäinen, J. P., O'Donnell, D., Teichmann, C., Karstens, U., Pfeifer, S., Kazil, J., Podzun, R., Fiedler, S., Kokkola, H.,

30 Birmili, W., O'Dowd, C., Baltensperger, U., Weingartner, E., Gehrig, R., Spindler, G., Kulmala, M., Feichter, J., Jacob, D. and Laaksonen, A.: The regional aerosol-climate model REMO-HAM. In: Geoscientific Model Development, 5(6), 1323-1339, 2012.

Pihlainen, S., Tahvonen, O. and Niinimäki, S.: The economics of timber and bioenergy production and carbon storage in Scots pine stands. Canadian Journal of Forest Research, 44(9): 1091-1102, https://doi.org/10.1139/cjfr-2013-0475, 2014.

Pingoud, K., Ekholm, T., Sievänen, T., Huuskonen, S. and Hynynen, J.: Trade-offs between forest carbon stocks and harvests in a steady state e A multi-criteria analysis. Journal of Environmental Management 210, 96-103, 2018.

Pudas, E., Leppälä, M., Tolvanen, A., Poikolainen, J., Venäläinen, A., and Kubin, E..: Trends in phenology of Betula pubescens across the boreal zone in Finland, International Journal of Biometeorology, 52, 251-259, 2008.

5 Pulliainen, J., M. Aurela, T. Laurila, T. Aalto, M. Takala, M. Salminen, M. Kulmala, A. Barr, M. Heimann, A. Lindroth, A. Laaksonen, C. Derksen, A. Mäkelä, T. Markkanen, J. Lemmetyinen, J. Susiluoto, S. Dengel, I. Mammarella, J.-P. Tuovinen and T. Vesala: Early snowmelt significantly enhances boreal springtime carbon uptake, Proceedings of the National Academy of Sciences Oct 2017, 201707889; DOI: 10.1073/pnas.1707889114, 2017.

Raddatz, T.J., Reick, C.H., Knorr, W., Kattge, J., Roeckner, E., Schnur, R., Schnitzler, K.G., Wetzel, P., Jungclaus, J.: Will
10 the tropical land biosphere dominate the climate-carbon cycle feedback during the twenty-first century?, Clim. Dyn., 29, 565–574, 2007.

Randerson, J.T., Liu, H., Flanner, M.G., Chambers, S.D., Jin, Y., Hess, P.G., Pfister, G., Mack, M.C., Treseder, K.K., Welp, L.R., Chapin, F.S., Harden, J.W., Goulden, M.L., Lyons, E., Neff, J.C., Schuur, E.A.G. and Zender, C.S.: The Impact of Boreal Forest Fire on Climate Warming, Science 314, 1130-1132, 2006.

15 Reick, C.H., Raddatz, T., Brovkin, V. and Gayler, V.: Representation of natural and anthropogenic land cover change in MPI-ESM., J. Adv. Model. Earth Syst., 5, 459–482, 2013.

Rinne, J., Aurela, M. and Manninen, T.: A Simple Method to Determine the Timing of Snow Melt by Remote Sensing with Application to the CO2 Balances of Northern Mire and Heath Ecosystems, Remote Sens., 1(4), 1097-1107, 2009.

Roesch, A., Wild, M., Gilgen, H. and Ohmura, A.: A new snow cover fraction parameterization for the ECHAM4 GCM.
20 Clim. Dyn., 17, 933–946, 2001.

Ruosteenoja, K., Jylhä, K and Kämäräinen, M.: Climate projections for Finland under the RCP forcing scenarios, Geophysica, 51(1), 17–50, 2016a.

Ruosteenoja, K., Räisänen, J., Venäläinen, A., Kämäräinen, M. and Pirinen, P.: Terminen kasvukausi lämpenevässä ilmastossa. Terra, (In Finnish with English summary), 128, 1: 3–15, 2016b.

25 Ruosteenoja, K.: Maailmanlaajuisiin ilmastomalleihin perustuvia lämpötila- ja sademääräskenaarioita. Sektoritutkimusohjelman ilmastoskenaariot (SETUKLIM) 1. osahanke, (In Finnish), Ilmatieteen laitos, 15 pp., 2013.

Räisänen, J. and Räty, O.: Projections of daily mean temperature variability in the future: cross-validation tests with ENSEMBLES regional climate simulations, Climate Dynamics, 41, 1553-1568, 2013.

Räisänen, P., Luomaranta, A., Järvinen, H., Takala, M., Jylhä, K., Bulygina, O. N., Luojus, K., Riihelä, A., Laaksonen, A.,
30 Koskinen, J., and Pulliainen, J.: Evaluation of North Eurasian snow-off dates in the ECHAM5.4 atmospheric general circulation model, Geosci. Model Dev., 7, 3037–3057, doi:10.5194/gmd-7-3037-2014, 2014.

Räty, O., Räisanen, J. and Ylhäisi, J.S.: Evaluation of delta change and bias correction methods for future daily precipitation: intermodel cross-validation using ENSEMBLES simulations, Climate Dynamics, 42, 2287-2303, 2014.

Salminen, S.: Eteläisimmän Suomen metsävarat 1986-1988 (In Finnish), Folia Forestalia 825, 1-116, 1993.

Salminen, S. and Salminen, O.: Metsävarat keskisessä Suomessa 1988-92 sekä koko Etelä-Suomessa 1986-92 (In Finnish), Metsäntutkimuslaitoksen tiedonantoja 710, 1998.

Shutova, E., Wielgolaski, F.E., Karlsen, S.R., Makarova, O., Berlina, N., Filimonova, T., Haraldsson, E., Aspholm, P.E., Flø, L., and Høgda, K.A.: Growing seasons of Nordic mountain birch in northernmost Europe as indicated by long-term field studies and analyses of satellite images, International Journal of Biometeorology, 51, 155-166, 2006.

Solantie, R., Drebs, A., Hellsten, E. and Saurio, P.: Lumipeitteen tulo-, lähtö- ja kestoajoista Suomessa talvina 1960/1961 – 1992/1993, ("On the beginning and end times and length of snow covered period in Finland in winters 1960/1961 – 1992/1993", in Finnish with English summary), Finnish Meteorological Institute, Meteorological publications No. 34, 159 pp., 1996.

Solantie, R.: Productivity of boreal forests in relation to climate and vegetation zones, Boreal Env. Res., 10, 275–297, 2005.

Solantie, R.: Growth of the South-Finnish Forests during the Period of 1961-2010 as Function of Thermal Conditions in Air and Soil, Baltic Forestry, 21(2), 219-232, 2015.

Sutinen, S., Roitto, M., Lehto, T. and Repo, T.: Simulated snowmelt and infiltration into frozen soil affected root growth, needle structure and physiology of Scots pine saplings, Boreal Env. Res., 19, 281–294, 2014.

Tanis, C.M, Peltoniemi, M., Linkosalmi, M., Aurela, M., Böttcher, K., Manninen, T. and Arslan, A.N.: A system for acquisition, processing and visualization of image time series from multiple camera networks. Data, 3(3), 23; doi: 10.3390/data3030023, 2018.

Teutschbein, C. and Seibert, J.: Bias correction of regional climate model simulations for hydrological climate-change impact studies: Review and evaluation of different methods, Journal of Hydrology, 456–457, 12-29, 2012.

Thackerey, S.J., Fletcher, C.G., Mudryk, L.R. and Derksen, C.: Quantifying the Uncertainty in Historical and Future Simulations of Northern Hemisphere Spring Snow Cover, J. Climate, 29(23), 8647-8663, 2016.

Tomppo, E., Heikkinen, J., Henttonen, H. M., Ihalainen, A., Katila, M., Mäkelä, H., Tuomainen, H., and Vainikainen, N.: Designing and Conducting a Forest Inventory-case: 9th National Forest Inventory of Finland: Designing and Conducting a Forest Inventory-Case: 9Th National Forest Inventory of Finland, Springer, 2011.

Tomppo, E., Henttonen, H., Ihalainen, A., Tonteri, T. and Tuomainen, T.: Etelä-Savon metsäkeskuksen alueen metsävarat 1966–2000 (In Finnish). Metsätieteen aikakauskirja 2B/2001: 309–388, 2001.

Tomppo, E., Henttonen, H., Korhonen, K.T., Aarnio, A., Ahola, A., Heikkinen, J., Ihalainen, A., Mikkelä, H., Tonteri, T. and Tuomainen, T.: Etelä-Pohjanmaan metsäkeskuksen alueen metsävarat ja niiden kehitys 1968–97 (In Finnish). Metsätieteen aikakauskirja – Folia Forestalia 2B/1998: 293–374, 1998.

Tomppo, E., Tuomainen, T., Heikkinen, J., Henttonen, H., Ihalainen, A., Korhonen, K.T., Mäkelä, H. and Tonteri, T.: Lapin metsäkeskuksen alueen metsävarat 1970–2003 (In Finnish). Metsätieteen aikakauskirja 2B/2005: 199–287, 2005.

Tomppo, E., Tuomainen, T., Henttonen, H., Ihalainen, A., Korhonen, K.T., Mäkelä, H. and Tonteri, T.: Pohjois-Pohjanmaan metsäkeskuksen alueen metsävarat 1968–2002 (In Finnish). Metsätieteen aikakauskirja 3B/2004: 339–418, 2004.

Tomppo, E., Tuomainen, T., Henttonen, H., Ihalainen, A. and Tonteri, T.: Kainuun metsäkeskuksen alueen metsävarat 1969–2001 (In Finnish). Metsätieteen aikakauskirja 2B/2003: 169–256, 2003.

Vihma, T.: Effects of Arctic Sea Ice Decline on Weather and Climate: A Review. Surv. Geophys. DOI 10.1007/s10712-014-9284-0, 2014.

Table 1. The regions based on the vegetation zones of Finland.

Region	Name	Type	Number of SAL pixels
1	Åland	Hemiboreal	3
2	Oak zone	Hemiboreal	19
3	Southwestern Finland	Southern boreal	127
4	Southern Ostrobothnia	Southern boreal	19
5	Lake district	Southern boreal	224
6	Northern Karelia – Kainuu	Middle boreal	112
7	Ostrobothnia	Middle boreal	212
8	Southwestern Lapland	Middle boreal	23
9	Kuusamo district	Northern boreal	47
10	North Ostrobothnia	Northern boreal	130
11	Northwestern Fjeld Lapland	Northern boreal	20
12	Forest Lapland	Northern boreal	86
13	Northern Fjeld Lapland	Northern boreal	30

Table 2. The regions based on the forest centres of Finland.

Region	Name	Mean solar zenith angle at onset of snow melt	Mean fraction of forested area [%]	Type	Number of SAL pixels
1	Åland	64.9°	59	Hemiboreal	40
2	Southern and Ostrobothnian coast	63.5°	62	Hemiboreal southern boreal	63
3	Southwestern Finland	63.7°	62	Hemiboreal - southern boreal	76
4	Häme – Uusimaa	62.4°	67	Southern boreal	52
5	Southeastern Finland	63.3°	74	Southern boreal	50
6	Pirkanmaa	62.9°	75	Southern boreal	48
7	Ostrobothnia	64.6°	70	Middle boreal	57
8	South Ostrobothnia		71	Middle boreal	71
9	Central Finland	61.3°	85	Middle boreal	64
10	Etelä-Savo	62.2°	85	Southern boreal	60
11	Pohjois-Savo	60.4°	81	Middle boreal	66
12	North Karelia	60.2°	84	Middle boreal	68
13	North Ostrobothnia	60.3°	77	Middle – Northern boreal	145
14	Kainuu	59.5°	87	Middle boreal	77
15	Southern Lapland	59.0°	81	Northern boreal	220
16	Northern Lapland	57.8°	51	Northern boreal	103

Table 3. Observed melt onset and melting season length trends during 1982 – 2015 from the CLARA-A2 SAL data of regions based on vegetation zones. The slope and coefficient of determination values are shown both for annual data and moving averages of five years. The cases for which the moving average of five years shows a significant coefficient of determination are indicated with bold fonts.

Region	Melt onset				Melting season length			
	Annual value		Moving average of five years		Annual value		Moving average of five years	
	Slope (Days per decade)	R^2	Slope (Days per decade)	R^2	Slope (Days per decade)	R^2	Slope (Days per decade)	R^2
Northern Fjeld Lapland	2.1	0.024	1.3	0.041	-6.3	0.097	-6.2	0.22
Forest Lapland	-0.03	0.0000067	-0.7	0.02	-1.5	0.0094	-1.4	0.033
Northwestern Fjeld Lapland	1.0	0.0076	0.6	0.014	-2.4	0.023	-3.1	0.13
North Ostrobothnia	-2.6	0.071	-3.3	0.33	3.9	0.12	4.3	0.44
Kuusamo district	-2.1	0.047	-3.3	0.34	3.0	0.052	4.7	0.35
Southwestern Lapland	**-4.7**	**0.17**	**-5.0**	**0.78**	**6.6**	**0.16**	**6.8**	**0.67**
Ostrobothnia	-3.5	0.083	-4.3	0.41	2.0	0.022	3.3	0.18
Northern Karelia - Kainuu	**-5.3**	**0.19**	**-6.3**	**0.81**	**5.8**	**0.12**	**7.1**	**0.68**
Lake district	-2.4	0.027	-3.7	0.23	-0.3	0.00038	1.7	0.028
Southwestern Finland	0.8	0.0027	-1.5	0.051	-6.4	0.098	-4.0	0.072

Table 4. Observed albedo trends of regions based on vegetation zones. The slope and coefficient of determination values are shown both for annual data and moving averages of five years. The cases for which the moving average of five years shows a significant coefficient of determination are indicated with bold fonts.

Region	Annual value		Moving average of five years	
	Slope (Albedo in % units per decade)	R^2	Slope (Albedo in % units per decade)	R^2
Northern Fjeld Lapland	-1.6	0.18	-1.8	0.36
Forest Lapland	**-2.3**	**0.52**	**-2.5**	**0.69**
Northwestern Fjeld Lapland	0.3	0.01	-0.2	0.01
North Ostrobothnia	**-3.4**	**0.72**	**-3.6**	**0.83**
Kuusamo district	**-3.1**	**0.66**	**-3.1**	**0.82**
Southwestern Lapland	**-3.3**	**0.61**	**-3.3**	**0.75**
Ostrobothnia	-1.4	0.23	-0.8	0.47
Northern Karelia - Kainuu	**-3.0**	**0.58**	**-2.6**	**0.84**
Lake district	-0.3	0.006	0.6	0.15
Southwestern Finland	0.2	0.004	0.5	0.06

Table 5. Observed albedo trends of regions based on forest centres. The slope and coefficient of determination values are shown both for annual data and moving averages of five years. The region Lapland is divided in northern and southern parts as shown in Figure 1. The cases for which the moving average of five years shows a significant coefficient of determination are indicated with bold fonts.

Region	Annual value		Moving average of five years	
	Slope (Albedo in % units per decade)	R^2	Slope (Albedo in % units per decade)	R^2
Lapland	**-2.7**	**0.60**	**-3.0**	**0.72**
Northern Lapland	-1.2	0.18	-1.5	0.40
Southern Lapland	**-3.3**	**0.70**	**-3.4**	**0.82**
North Ostrobothnia	**-2.1**	**0.48**	**-1.7**	**0.75**
Central Finland	-0.05	0.0001	0.9	0.19
Etelä-Savo	-0.5	0.01	0.4	0.06
Pirkanmaa	0.6	0.02	1.3	0.30
Southwestern Finland	0.5	0.007	1.3	0.11
Southeastern Finland	-0.2	0.002	0.6	0.08
Häme – Uusimaa	0.4	0.009	0.3	0.05
Kainuu	**-3.0**	**0.58**	**-2.8**	**0.81**
South Ostrobothnia	-0.5	0.02	0.03	0.0003
Pohjois-Savo	-1.1	0.07	-0.6	0.11
North Karelia	**-1.9**	**0.24**	**-1.3**	**0.53**

Figure 1. The regions based on the vegetation zones (left) and the regions of the forest centres (right) of Finland. The Finnish territory (including islands) is situated between the latitudes 59.5 N and 70.1 N and the longitudes 19.1 E and 31.6 E.

Figure 2. Examples of sigmoid fitting. Original data points are shown in blue, the fit in red and the data points from which vegetation greening effect has been removed in black. a) initial fit of an easy case, b) final fit of the easy case, c) initial fit of a case with strong influence of vegetation greening on albedo, d) final fit of the case with strong influence of vegetation greening on albedo.

Figure 3. Optimal values of k as a function of the fraction of the forested area in the forest centre area (f). The brown point is not included in the regression $k = 0.11 + 1347.44 \exp(-11\,f)$, because it represents an area dominated by deciduous species (mountain birch).

Figure 4. The melt onset day of the snow cover in Finland during 1982 – 2011 based on CLARA-A2 SAL product and JSBACH model snow depth.

Figure 5. Trends of the melt onset day of the snow cover in Northern Karelia – Kainuu and Northern Ostrobothnia during 1982 – 2015 based on CLARA-A2 SAL product. The solid curves represent the five year moving averages and the dotted curves the annual values.

Figure 6. Comparison of diverse estimates of the melt-off day of snow cover. The FMI snow maps of end of permanent snow cover are based on in situ snow depth measurements. The satellite based melt-off date estimates are derived using the surface albedo product CLARA-A2 SAL (Anttila et al., 2016, Karlsson et al., 2017) and the FSC snow product calculated from MODIS images (Metsämäki et al., 2018). The JSBACH model estimate of end of snow melt is also shown. For comparison the greening-up date of deciduous vegetation (SYKE DEC; Böttcher et al., 2016) is also presented.

Figure 7. The proceeding of spring in 2006 and 2012 starting from a & e) the melt-off day of the permanent snow cover in Finland based on *in situ* snow depth measurements (Solantie et al., 1996; Kersalo and Pirinen, 2009), b & f) the surface albedo reaching the 20 % threshold value of its dynamic range during the melting season (Anttila et al., 2016, Karlsson et al., 2017), c & g) the complete disappearance of the snow cover based on the FSC product (Metsämäki et al., 2018) and d & h) the greening-up day based on MODIS NDWI (Böttcher et al., 2016).

Figure 8. Trends of the melting season length of the snow cover in Northern Karelia – Kainuu and Northern Ostrobothnia during 1982 – 2015 based on CLARA-A2 SAL product. The solid curves represent the five year moving averages and the dotted curves the annual values.

Figure 9. The surface albedo (%) at the time of the melt onset in Finland. The average value during 1982-1986 (left), during 1982-2015 (middle) and during 2011-2015 (right). The black pixels in Finland represent cases, when the melting has already started before the albedo could be retrieved, i.e. when the sun zenith angle was larger than 60°.

Figure 10. Comparison of observed albedo variation (colour solid curves) of the forest centre areas (Figure 1, Table 2) during 1982 – 2015 and corresponding albedo model results based on stem volume measurements (points). The interpolation curves (grey solid curves) of the modelled annual values are shown as well. The colours match those of the map in Figure 1b, except for Lapland, which is treated as one area (15 and 16).
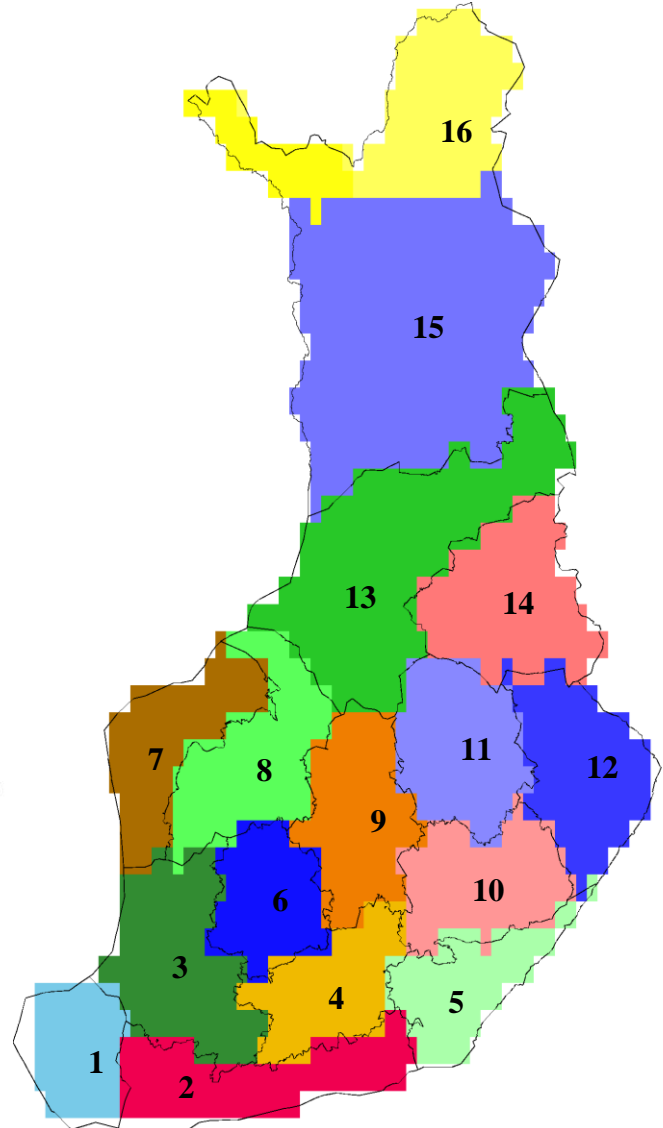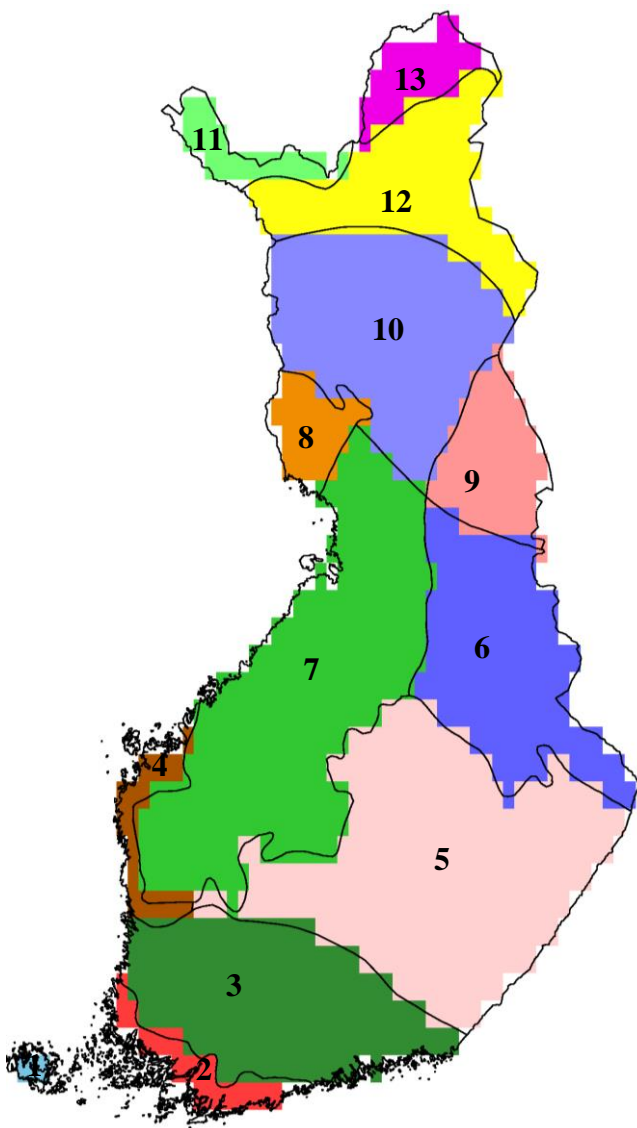
Figure 1
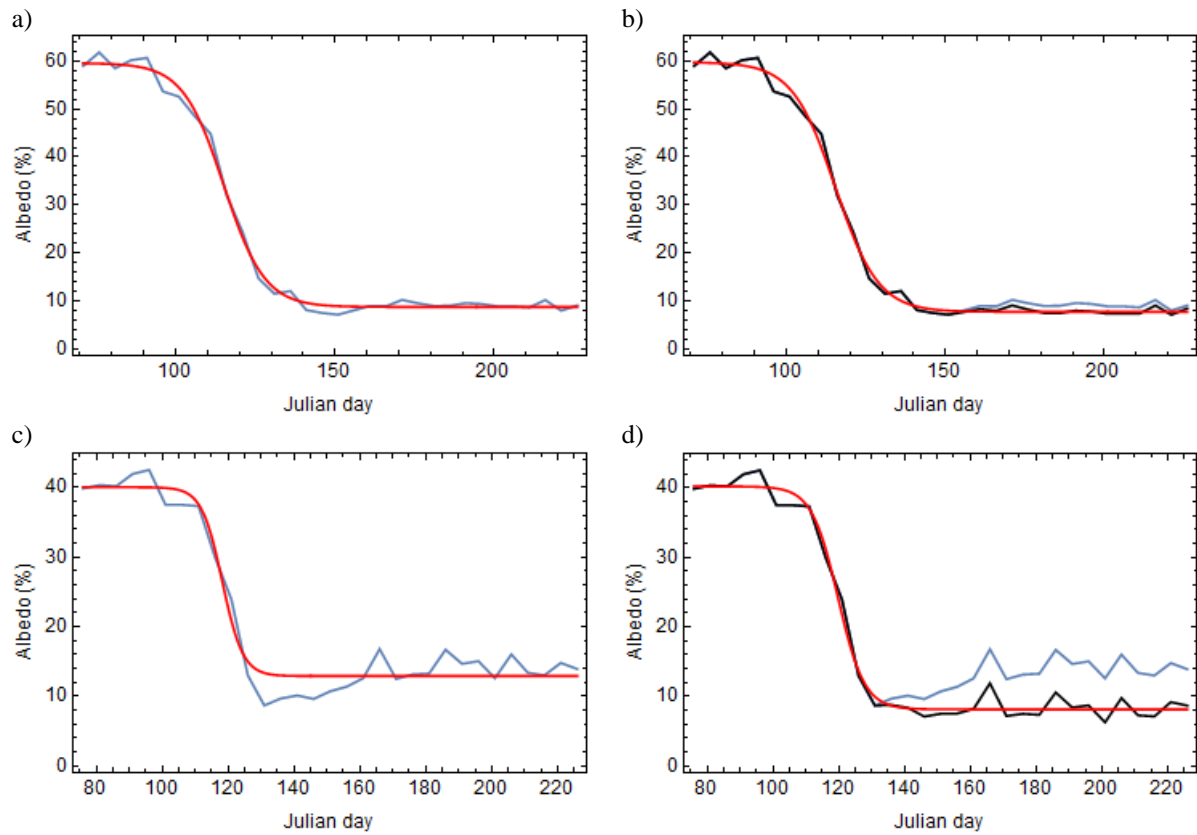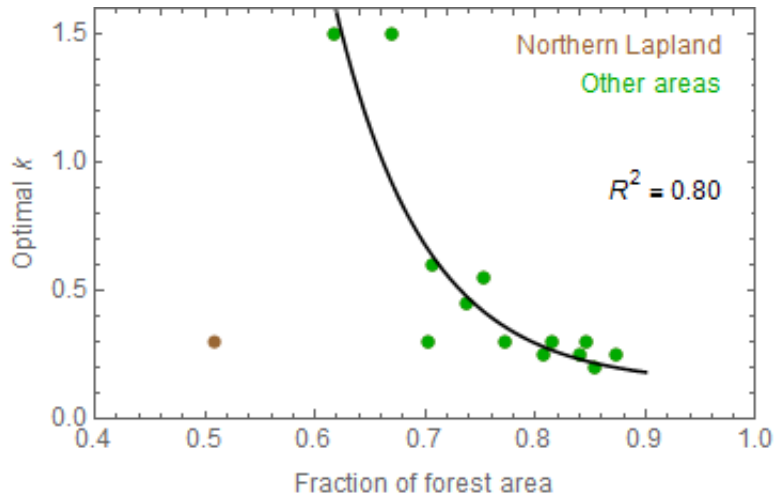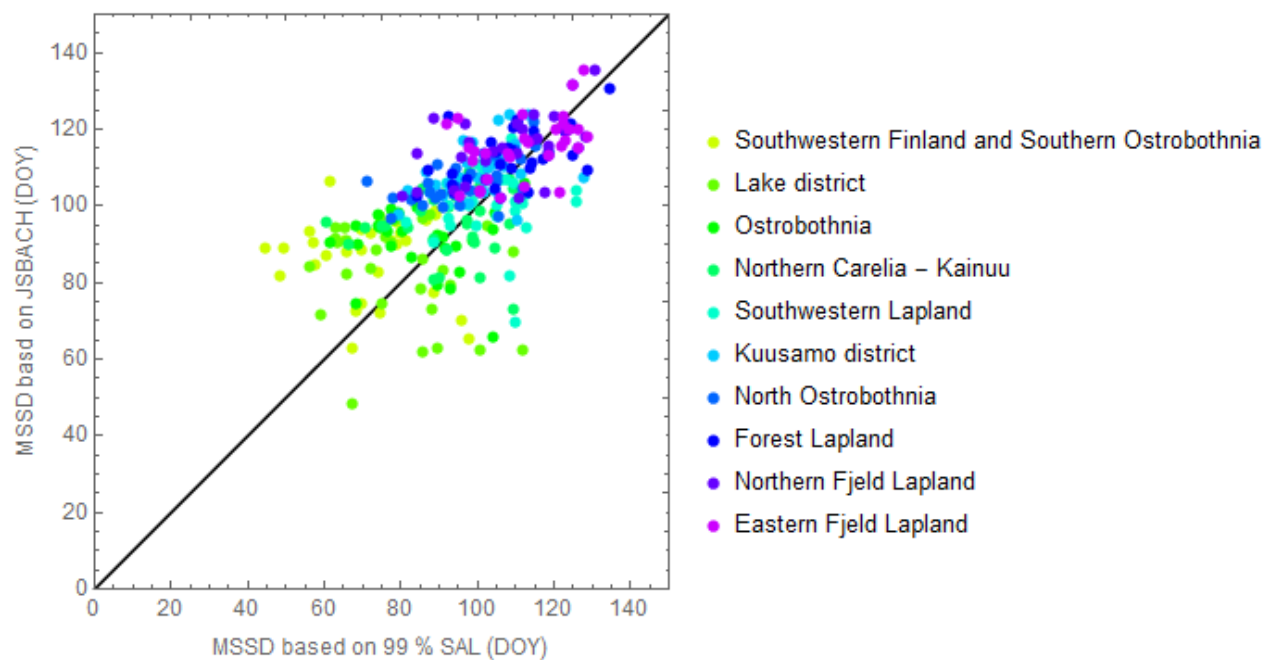
Figure 2

Figure 3

Figure 4
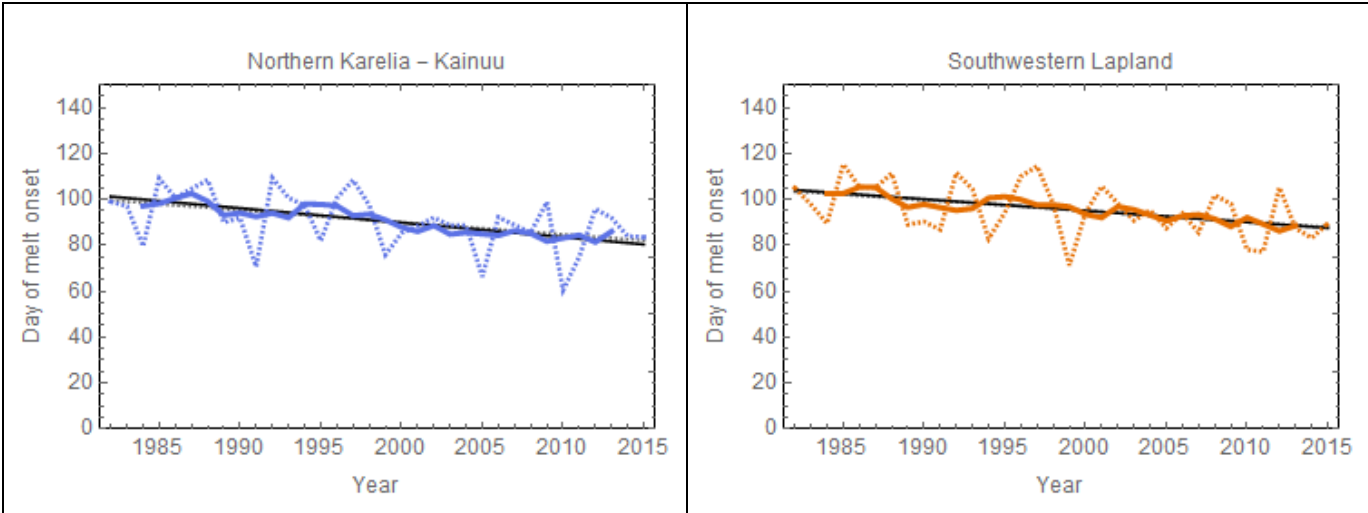
Figure 5
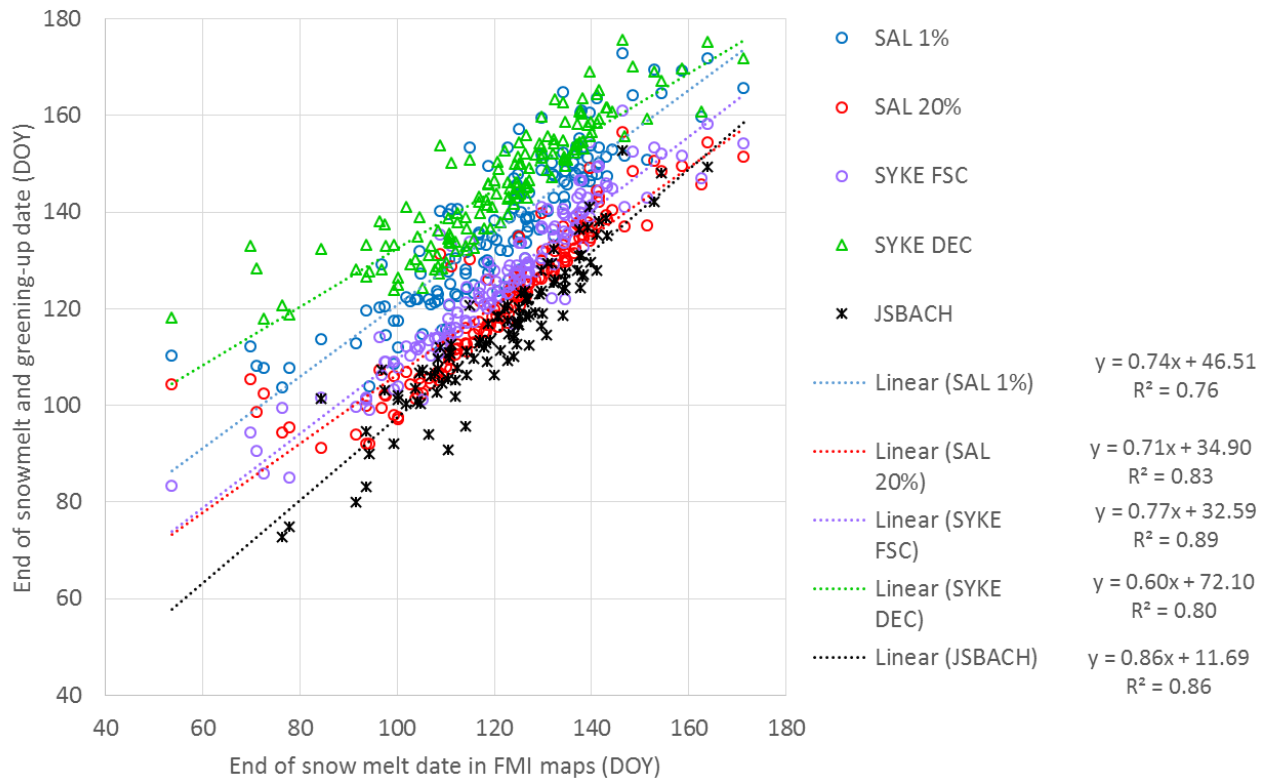
Figure 6
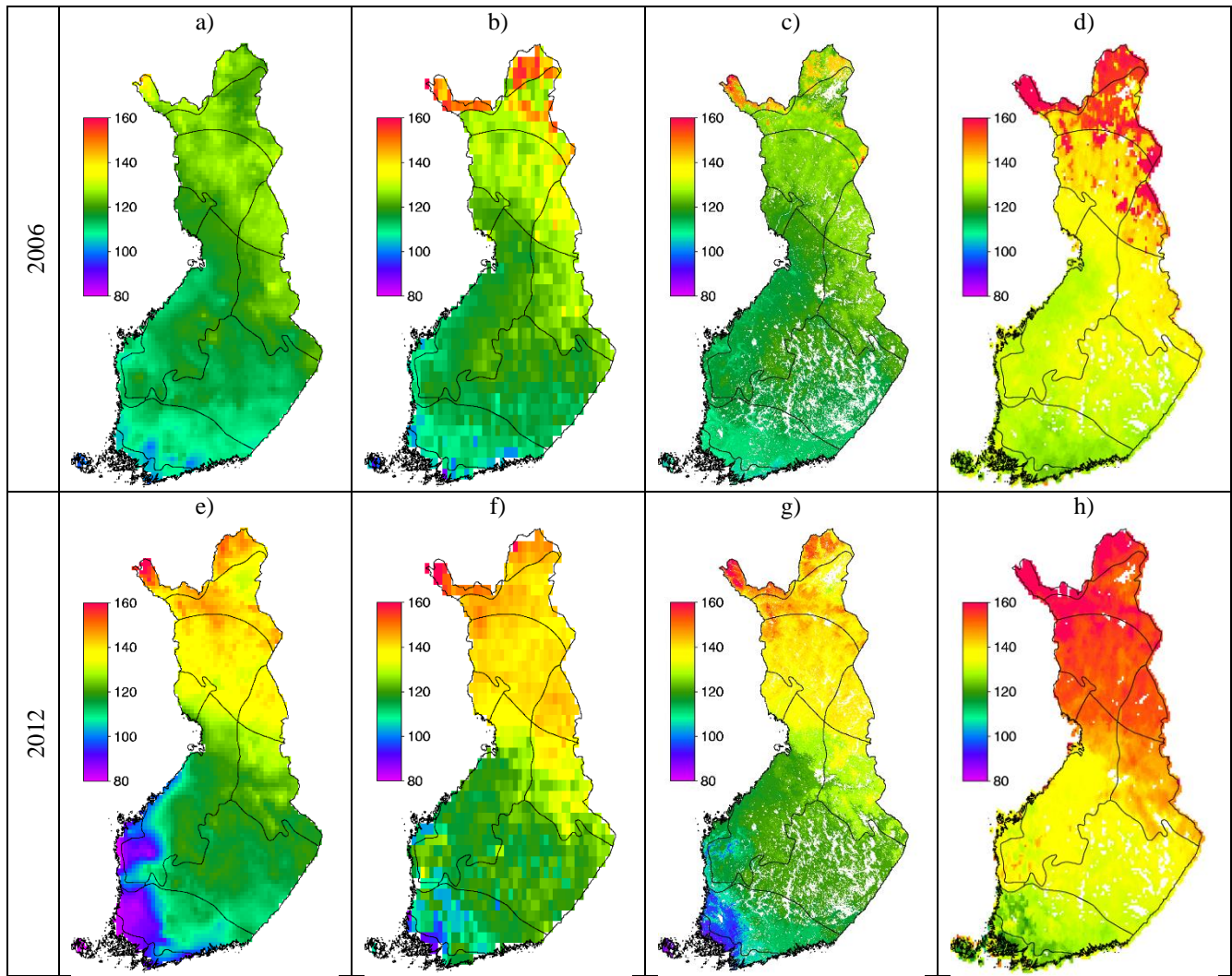
Figure 7
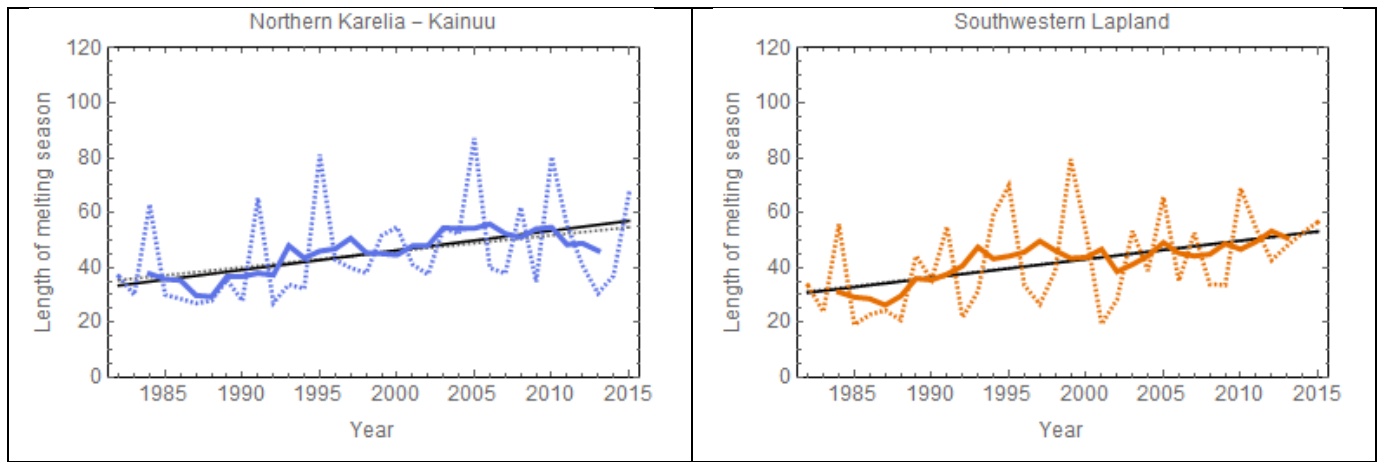
Figure 8

Figure 9

Figure 10